2010

Magnetic anisotropy in itinerant magnets

Ralph Skomski
University of Nebraska-Lincoln, rskomski2@unl.edu

Arti Kashyap
LNM Institute of Information Technology, Jaipur-302031, Rajasthan, India, akashyap@lnmiit.ac.in

A. Solanki
Malaviya National Institute of Technology, Jaipur-302017, Rajasthan, India

Axel Enders
University of Nebraska-Lincoln, a.enders@me.com

David J. Sellmyer
University of Nebraska-Lincoln, dsellmyer@unl.edu

Magnetic anisotropy in itinerant magnets

R. Skomski,[1,a)] A. Kashyap,[2] A. Solanki,[3] A. Enders,[1] and D. J. Sellmyer[1]
[1]*Department of Physics and Astronomy and Nebraska Center for Materials and Nanoscience, University of Nebraska, Lincoln, Nebraska 68588, USA*
[2]*LNM Institute of Information Technology, Jaipur-302031, Rajasthan, India*
[3]*Malaviya National Institute of Technology, Jaipur-302017, Rajasthan, India*

(Presented 20 January 2010; received 31 October 2009; accepted 19 December 2009; published online 30 April 2010)

The structural dependence of the magnetocrystalline anisotropy of itinerant permanent magnets (or nanostructures of iron-series 3*d* elements) is investigated by model and tight-binding calculations. Magnetic nanostructures yield strong oscillations of the anisotropy as a function of the number of *d* electrons per atom, which can be tuned by alloying. While interatomic hopping is usually more important in metals than crystal-field interactions, we find substantial crystal-field corrections for some configurations, especially for the atomic square. Finally, we compare our results with Néel model. © *2010 American Institute of Physics*. [doi:10.1063/1.3339780]

I. INTRODUCTION

A key question in permanent magnetism is the prediction of the magnetocrystalline anisotropy from the atomic structure. For rare-earth transition-metal magnets, reasonable estimates are obtained by evaluating the crystal-field (CF) interactions of the rare-earth ions.[1,2] This is possible because the spin-orbit coupling is sufficiently strong to rigidly couple the rare-earth spins to the aspherical charge distribution of the 4*f* shell. As a consequence, the anisotropy energy is equal to the electrostatic energy of this charge distribution in the CF. The understanding of structure-property relationships for itinerant 3*d*, 4*d*, and 5*d* anisotropies is much less developed, despite the fact that the basic relationship between CF or band-structure level splitting, spin-orbit coupling, and anisotropy has been known for almost a century.[3] It is possible to calculate the anisotropy numerically,[4,5] but there are no rules predicting how atomic substitutions change the anisotropy of rare-earth-free permanent magnets. In the past, such substitutions have played an important role in the development of permanent magnets, as exemplified by the role of interstitial carbon in hard-magnetic steel. Similarly, some layered W-Fe structures have benn predicted to be magnetically very hard,[6] and the same is true for tetragonally distorted Fe–Co alloys.[7]

Both rare-earth and itinerant anisotropies are largely single-ion, that is, each *d* atom yields an individual anisotropy contribution determined by the atom's spin-orbit interaction. Fuchikami[8] determined the magnetocrystalline anisotropy of $BaFe_{12}O_{19}$ from the CF interaction of the trigonal iron site. However, in transition-metal alloys, the interatomic hopping is much larger than the crystal-field splitting and band-structure calculations are a better starting point for the understanding of the anisotropy. The CF interaction, which affects the on-site energy of the orbitals, is sometimes considered as the leading consideration in transition-metal oxides,[3,8,9] but interatomic hopping is also important in oxides.[10,11]

II. BAND-STRUCTURE EFFECTS

Let us investigate the itinerant anisotropy of iron-series transition-metal magnets on a tight-binding level. Due to the Bloch symmetry, second-order perturbation theory amounts to a single *k*-space integration over $1/[E_\mu(\mathbf{k})-E_\nu(\mathbf{k})]$, where μ and ν are subband indices. During the integration or summation, the Fermi level (or HOMO-LUMO bital gap between the highest occupied and lowest unoccupied orbitals) is between $E_\mu(\mathbf{k})$ and $E_\nu(\mathbf{k})$. However, as illustrated in Fig. 1, there are regions in **k**-space where $E_\mu(\mathbf{k}) \approx E_\nu(\mathbf{k}) \approx E_F$ and perturbation theory breaks down. If these states are at the Fermi level, denoted by the small circle in Fig. 1, then they yield a disproportionally strong anisotropy contribution.[12]

The corresponding anisotropy contribution depends on the quantum number *m* of the involved states,[2] but for nearly degenerate states of level spacing ε it is of order

$$K_1 = \frac{1}{V_{at}}\left(\sqrt{\frac{\varepsilon^2}{4}+\lambda^2}-\frac{\varepsilon}{2}\right). \quad (1)$$

Here, λ is the spin-orbit coupling constant (about 50 meV for Fe, Co, and Ni) and V_{at} is the atomic volume. For perfectly degenerate levels ($\varepsilon=0$), Eq. (1) reduces to $K_1=\lambda/V_{at}$, where is the crystal volume per transition-metal atom. This is a huge anisotropy, about 500 MJ/m^3 [5 $Gergs/cm^3$], and despite the limited number of such **k**-states, the net effect is not necessarily small,[12] especially for layered and chainlike

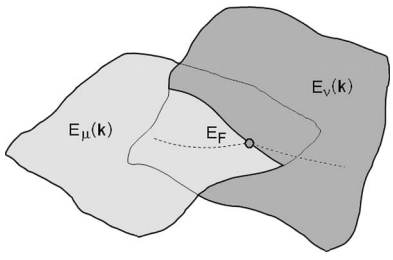

FIG. 1. Energy landscape and degenerate states. In two and three real-space dimensions, $E(\mathbf{k}_\mu)=E(\mathbf{k}_\nu)=E_F$ yields zero and one-dimensional spaces, respectively.

a)Electronic mail: rskomski@neb.rr.com.

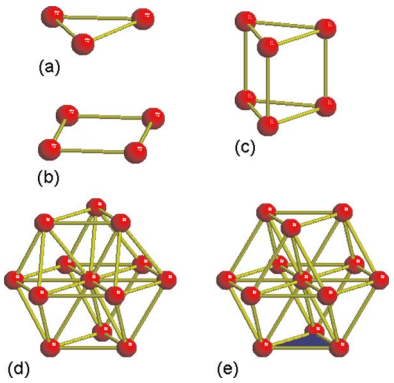

FIG. 2. (Color online) Typical transition-metal clusters.

atomic configurations. In the limit of well-separated levels ($\varepsilon \gg \lambda$), Eq. (1) reduces to the second-order perturbation result $K_1 V_{at} = \lambda^2/\varepsilon$. Since the spacing between randomly chosen levels is of the order of the band width W, this can also be written in the well-known form $K_1 V_{at} \sim \lambda^2/W$.

The total anisotropy is obtained by summation or integration over all pairs of levels. Our phenomenological but nonperturbative $3d$ tight-binding calculation yields the anisotropies for the clusters shown in Fig. 2 as a function of the number n of $3d$ electrons per atom (d count). Experimentally, n can be varied by alloying, similar to the control of the magnetization on the Slater–Pauling curve. Figure 3 shows the result for the hexagonal cluster of Fig. 2(d). While the present non-self-consistent $3d$-only tight-binding method cannot be expected to yield accurate peak heights and positions, the main feature of Fig. 3, namely, the occurrence of a large number of peaks and zeros, is unaffected by the present approximations. The oscillations occur in the hcp cluster but not in the fcc cluster because the former has a twofold axis of symmetry. In the fcc cluster, it is not possible to define such a twofold axis because the a, b, and c directions are equivalent.

The surprising feature is not the well-known existence of peaks and zeros, but their larger number of the peaks, even for the relatively simple structure of Fig. 2(d). It is therefore not surprising that the anisotropy of typical transition-metal alloys, such as fcc-based $Co_{1-x}Ni_x$ and $Fe_{1-x}Ni_x$, is a nonlinear function of the concentration x, in spite of some averaging due to atomic disorder.

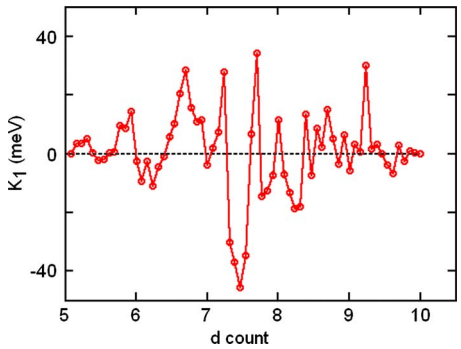

FIG. 3. (Color online) Anisotropy of the hexagonal cluster of Fig. 2(d) as a function of the number n of d electrons per atom. For the corresponding fcc cluster [Fig. 2(e)], $K_1 = 0$.

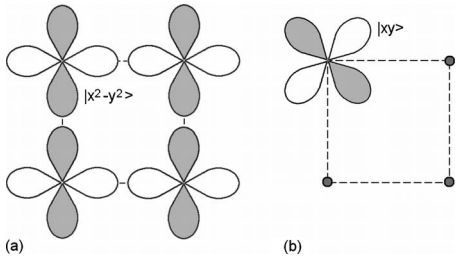

FIG. 4. Lowest-lying $|m|=2$ levels: (a) bonding state created by interatomic hybridization and (b) CF state. The hybridization involves $|x^2-y^2\rangle$ orbitals because the magnitude of the corresponding hopping integral $(3V_{dd\sigma} + V_{dd\delta})/4$ is larger than that of the integral $V_{dd\pi}$ connecting $|xy\rangle$ states. The lower CF energy of the $|xy\rangle$ level reflects the sign of typical CF charges. These charges are usually negative, with hydrogen and possibly boron in very electronegative environments being the only exceptions (Ref. 14), so that the negatively charged $3d$-electron lobes avoid neighboring atoms.

While the clusters of Figs. 2(d) and 2(e) are structurally very similar, their anisotropies hugely differ, with large (Fig. 3) and zero second-order anisotropies, respectively. The underlying structural difference is the rotation of the bottom triangle, dark gray in Fig. 2(e), relative to the top triangle.

III. CRYSTAL-FIELD EFFECTS

From a basic point of view, it does not matter whether the isotropic levels correspond to localized CF levels or to extended states (linear combination of atomic orbitals or Bloch states). In chemistry, a similar distinction is made between electrostatic CF interaction and ligand-field theory, respectively.[13] However, specific level predictions strongly depend on the interaction mechanism. Figure 4 illustrates this point by considering the lowest-lying one-electron state formed from the $|xy\rangle$ and $|x^2-y^2\rangle$ orbitals on the square of Fig. 2(d). Interatomic hopping favors strongly bonding $|x^2-y^2\rangle$ states, whereas the CF interaction favors $|xy\rangle$ states.

Of course, interatomic hopping dominates in metals, and one might expect that the CF interaction is negligible. In fact, the full tight-binding analysis of Fig. 2(d) yields a strong easy-axis anisotropy contribution perpendicular to the square, caused by the strong spin-orbit induced hybridization of the orbitals shown in Figs. 5(a) and 5(b). This is possible because the two states in Fig. 5 have the same number of bonding and antibonding orbitals, so that the states are degenerate ($\varepsilon = 0$) and Eq. (1) predicts a huge anisotropy. However, the CF enhances the energy of the (a) $|x^2-y^2\rangle$ orbitals relative to that of the (b) $|xy\rangle$ orbitals. The effect is described

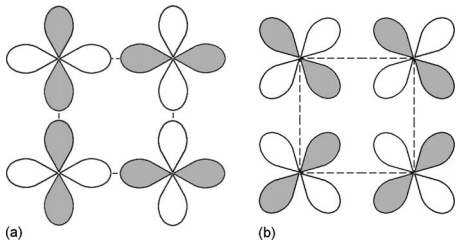

FIG. 5. Pair of molecular orbitals that yield a strong anisotropy contribution perpendicular to the square: (a) hybridization of $|x^2-y^2\rangle$ orbitals and (b) hybridization of $|xy\rangle$ orbitals.

by Eq. (1), except that $m=2$ requires the replacement of λ by 2λ. Taking $\lambda=0.05$ eV and $\varepsilon=0.2$ eV yields an anisotropy reduction by 59%.

IV. DISCUSSION AND CONCLUSIONS

An atomic model frequently used to discuss itinerant anisotropies is the Néel model.[15,16] However, the Néel model assumes a pair interaction between two magnetic atoms and is unable to describe the effect of nonmagnetic atoms, which affect the anisotropy by altering CF, level occupancy, and interatomic hopping. In $L1_0$ type magnets, such as PtCo and PdFe, the Néel model is also unable to distinguish between two important anisotropy contributions, namely, the large $4d/5d$ anisotropy caused by $3d$ neighbors and the $3d$ anisotropy created by the noncubic $4d/5d$ environment.[17] The latter is a rather traditional and fairly weak mechanism, whereas the former means that spin-polarized $3d$ electrons hop into $4d/5d$ orbitals and create substantial anisotropy by partly spin-polarizing the $4d/5d$ electrons, which exhibit a strong spin-orbit coupling.

Interestingly, neither CF nor Néel interactions explain the anisotropy difference between the hcp and fcc clusters of Figs. 2(d) and 2(e), respectively, because the coordination angles with respect to the c-axis (z-axis) are the same. This shows that more distant neighbors are very important. Alternatively, the peaks in Fig. 3 mean that small energy differences must be resolved properly, which requires the consideration of many neighbors.

The models of Sec. II are similar to the diatomic pair model[18] but go beyond perturbation theory. In fact, degenerate levels with huge anisotropy contributions, such as those of Fig. 5, also occur in the pair model but are ignored in Ref. 18. This is another example of level degeneracies having a strong effect on the magnetic anisotropy.

Our results indicate that rules for $3d$ anisotropies are difficult to establish and will probably have many exceptions. However, there are a few trends. For example, nearly filled d bands (Ni, Pd, and Pt) tend to yield anisotropy parallel to the pair axis. This corresponds very roughly to the peak above $n=9$ in Fig. 3 and is consistent with the magnetically easy $3d$-$4d/5d$ bond direction in $L1_0$-ordered FePt and CoPt. The reason is the pronounced σ character of the antibonding d orbitals near the upper edge of the conduction band. The creation of one hole per atom removes these $m=0$ states and leaves an excess of electrons that support an easy axis parallel to the bond axis.

In conclusion, we have inversitgated how structural and stoichiometric changes affect the magnetocrystalline anisotropy of itinerant magnets. Seemingly minor changes, extending beyond next neighbors, may have a strong impact on the anisotropy, and further research is necessary to see whether and how such effects can be exploited in new transition-metal based permanent-magnet materials.

ACKNOWLEDGMENTS

Thanks are due to V. Sharma, P. Sahota, and P. Manchanda for discussing various aspects of numerical anisotropy calculations. This work is supported by NSF MRSEC (R.S. and A.E.), ONR (R.S.), DST (A.K.), and DOE (D.J.S.).

[1] J. F. Herbst, Rev. Mod. Phys. **63**, 819 (1991).
[2] R. Skomski and J. M. D. Coey, *Permanent Magnetism* (Institute of Physics, Bristol, 1999).
[3] F. Bloch and G. Gentile, Z. Phys. **70**, 395 (1931).
[4] H. Brooks, Phys. Rev. **58**, 909 (1940).
[5] S. Willoughby, J. MacLaren, T. Ohkubo, S. Jeong, M. E. McHenry, D. E. Laughlin, S.-J. Choi, and S.-J. Kwon, J. Appl. Phys. **91**, 8822 (2002).
[6] T. Andersen and W. Hübner, Phys. Rev. B **74**, 184415 (2006).
[7] T. Burkert, L. Nordström, O. Eriksson, and O. Heinonen, Phys. Rev. Lett. **93**, 027203 (2004).
[8] N. Fuchikami, J. Phys. Soc. Jpn. **20**, 760 (1965).
[9] H. Bethe, Ann. Phys. **395**, 133 (1929).
[10] L. F. Mattheiss, Phys. Rev. B **5**, 290 (1972); **5**,306 (1972).
[11] W. L. Roth, Phys. Rev. **110**, 1333 (1958).
[12] A. Lessard, T. H. Moos, and W. Hübner, Phys. Rev. B **56**, 2594 (1997).
[13] C. J. Ballhausen, *Ligand Field Theory* (McGraw-Hill, New York, 1962).
[14] D. J. Newman and B. Ng, Rep. Prog. Phys. **52**, 699 (1989).
[15] L. Néel, J. Phys. Radium **15**, 225 (1954).
[16] D. S. Chuang, C. A. Ballentine, and R. C. O'Handley, Phys. Rev. B **49**, 15084 (1994).
[17] R. Skomski, A. Kashyap, and D. J. Sellmyer, IEEE Trans. Magn. **39**, 2917 (2003).
[18] D.-Sh. Wang, R.-Q. Wu, and A. J. Freeman, Phys. Rev. B **47**, 14932 (1993).